Preprint version of the manuscript: Manuel Lara, Mario L. Ruz, Iñaki Sandua, Franciso Vázquez, Juan Garrido, Optimal Active Generator Torque Control Strategies for Tower Lateral Load Reduction in the IEA 15 MW Wind Turbine, 11th Congress of the Federation of Simulation Societies in Europe (EURSIM 2023); Simulation for a Sustainable Future. Amsterdam, (The Netherlands), julio 2023, pp. 1-6, doi: 10.11128/arep.23. ARGESIM Report no. 23 – ISBN 978-3-903347-63-2, ARGESIM Publisher – Vienna.

Optimal Active Generator Torque Control Strategies for Tower Lateral Load Reduction in the IEA 15 MW Wind Turbine

***Manuel Lara. **Mario L. Ruz. ***Iñaki Sandua. *Francisco Vázquez. *Juan Garrido**

**Department of Electrical Engineering and Automation, University of Cordoba, Campus of Rabanales, Cordoba, Spain (email: p12laorm@uco.es, juan.garrido@uco.es, fvazquez@uco.es)*

***Department of Mechanics, University of Cordoba, Campus of Rabanales, Cordoba, Spain (email: mario.ruz@uco.es)*

****National Renewable Energy Centre (CENER), Ciudad de la Innovación, 7, Sarriguren, 31621, Spain (email: isandua@cener.com)*

Abstract: The extension of wind turbines' lifetime by reducing fatigue loads is a topic of interest. The contribution of this work is focused on designing a controller that mitigates lateral tower vibrations in the full load region. The proposed strategy is based on Active Generator Torque Control (AGTC), which produces an extra component of the generator torque added to the rated torque. In addition, the AGTC control is combined with a Collective Pitch Control (CPC) scheme based on the NREL's Reference OpenSource Controller (ROSCO), whose main purpose is to reject wind speed perturbation maintaining the wind turbine speed at its nominal value. Some variants of this scheme are proposed including an optional filter and a derivative gain in the AGTC. The controller parameter tuning is formulated as an optimization problem that minimizes the Fatigue Damage Equivalent Load (DEL) index for tower lateral loads. The resolution is carried out through genetic algorithms, and the design is applied to the IEA 15 MW RWT wind turbine model developed by NREL using the OpenFAST software. The ROSCO controller is used as the baseline scheme, comparing its performance with the proposed AGTC+CPC schemes. According to the simulation results, all the proposed AGTC strategies reduce the DEL index more than 30% with respect to the baseline controller. This reduction can be increased up to 42% at the expense of higher oscillations in the generated power and torque signal.

Keywords: lateral tower vibration control; vibration load mitigation; IEA 15 MW wind turbine

1. INTRODUCTION

Avoiding the dangers of climate change is a priority for the European Union, which is working hard to significantly reduce its greenhouse gas emissions, encouraging other states and regions to do the same. Renewable energy sources such as wind, water and solar energy are becoming increasingly important due to the lower impact on the environment. Considering that about 30% of greenhouse gas emissions are due to the production of electricity, wind energy has had a great boost due to its little negative impact on the environment (Njiri & Söffker, 2016).

Currently, horizontal axis wind turbines with three blades and variable speed and variable blade pitch (VS-VP) are the most common because they can optimize power generation at various wind speeds (Gambier, 2021). VS-VP wind turbines operate in different modes or regions depending on the wind speed: cut-in (I), partial load (II), transition (III), full load (IV), and cut-out (V), as shown in Fig. 1, which displays the ideal power curve of the wind turbine.

This research focuses on region IV (full load region), where the high wind speed's impact must be minimized to prevent damage to the system. In this case, it is necessary to maintain the generator power and, consequently, the generator speed at their nominal values. This is achieved through controllers that act on the blade pitch angle to adjust the wind turbine's aerodynamics and limit the amount of energy extracted from the wind (Novaes et al., 2018). In this region, the generated power (P_g) depends solely on the generator speed, ω_g, according to (1), since the generator torque is maintained constant at its rated value.

$$P_g = T_{g,rated} \cdot \omega_{g,rated} \quad (1)$$

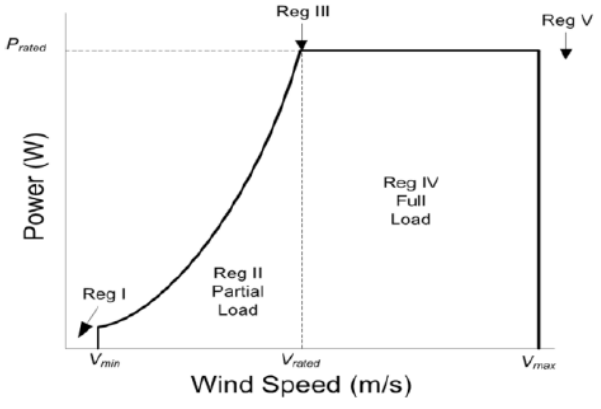

Figure 1. Operation region of a wind turbine.

The negative consequences of structural loads (particularly those brought on by aerodynamic and gravitational forces) become worse as wind turbines get bigger and more powerful. Structural loads that are not reduced might result in poor performance or even early failure of the entire wind turbine system. Therefore, it is crucial to understand how structural stresses interact, impact wind turbine power output, and alter the longevity of the device. The diverse deflection modes in the tower and rotor blades, or vibrations in the turbine drive train, are the most frequent occurrences that might result in various forms of structural stresses (Njiri & Söffker, 2016).

The tower structure mainly shows two vibration modes: fore-aft and side-side. Most of the research carried out focused on mitigating the fore-aft tower vibrations (Liu et al., 2016; Mohammadi et al., 2018). In Niranjan & Ramisetti (2022), a finite element structural analysis was combined with an active Tuned Mass Damper (TMD) to reduce the fore-aft vibration of a monopile-supported offshore wind turbine. In Gambier et al. (2022), a collective pitch control (CPC) is combined with an active tower damping control (ATDC) for a large wind turbine and both control loops are tuned together.

Lateral vibrations (i.e., side-side) in horizontal axis wind turbine towers can be caused by wind-induced vibration loads. There are three main categories of methods for controlling excessive vibrations in engineering structures when subjected to external vibrations: passive, semi-active, and active (Zuo et al., 2020). This paper is focused on designing a controller that mitigates lateral tower vibrations in the full load region. The remainder of this paper is organized as follows: Section 2 contextualizes this work, providing some background about loads in wind turbines and their control. In Section 3, the proposed control scheme is described, including the parameter tuning procedure. Section 4 shows the simulation results of the proposed controller, and the improvements are commented. Finally, the conclusions are summarized in Section 5.

2. BACKGROUND

2.1 Control approaches for tower lateral vibrations

Regarding control approaches for tower lateral vibrations, some investigations have been carried out with passive control methods to reduce lateral vibrations of the tower. In Liu et al., (2022), a spring pendulum pounding tuned mass damper was developed to mitigate the lateral response of monopile offshore wind turbines. In Zhang et al., (2016), the performance of full-scale tuned liquid dampers to mitigate lateral tower vibrations of multi-megawatt wind turbines was evaluated using real-time hybrid testing. These types of devices (i.e., TMDs and their variants) can either be fully passive or semi-actively controlled (Mensah and Dueñas-Osorio, 2014).

On the other hand, results of research papers on active structural control of wind turbines (Lackner & Rotea, 2011) show that active control is a more effective way of reducing structural loads than passive and semi-active control methods, at the cost of higher energy input and consequently a more expensive method. For example, Zhang et al. (2014) proposed an active generator-torque control (AGTC) to compensate for lateral tower vibrations, demonstrating AGTC can provide damping to these oscillations. The generator torque affects the side-side tower vibrations through the reaction on the generator stator, which is rigidly fixed to the nacelle. In Golnary & Tse (2022), a fuzzy torque control and a sliding mode pitch controller are developed to reduce power output fluctuations and tower lateral oscillations simultaneously.

2.2 Wind turbine model and simulation environment

In this study, a wind turbine model is simulated using the MATLAB/Simulink software with the assistance Fatigue, Aerodynamics, Structures, and Turbulence (OpenFAST) software (OpenFast, 2022). The International Energy Agency (IEA) Wind 15-Megawatt Reference Wind Turbine used in this work is being recently reported in the literature (Niranjan & Ramisetti, 2022; Papi & Bianchini; 2022). The turbine is available on GitHub (NREL, 2020). In this work, the turbine is configured in its land-based version. The main specifications are presented in Table 1.

Table 1. Properties of the IEA 15 MW RWT

Property	Value
Power rating	15 MW
Rotor orientation, configuration	Upwind, 3 blades
Cut-In, Rated Rotor Speed	5 rpm, 7.56 rpm
Cut-In, Rated, Cut-Out Wind Speed	3 m/s, 10.59 m/s, 25 m/s
Drivetrain	Low speed. Direct drive
Rated Generator Torque	19786767.5 Nm
Electrical Generator Efficiency	95.756%
Rotor, Hub Diameter, Hub height	240 m, 7.94 m, 150 m
Rotor nacelle assembly mass	1070000 kg
Tower Mass	860000 kg
Limits on the blade pitch angle	0 – π/2 rad
Slew-rate limits on the pitch actuator	0.0349 rad/s
Slew-rate limits on the generator torque	4500000 Nm/s

Fig. 2 shows the steady-state performance of the rotor as a function of wind speed, using OpenFAST with ROSCO (NREL, 2019).

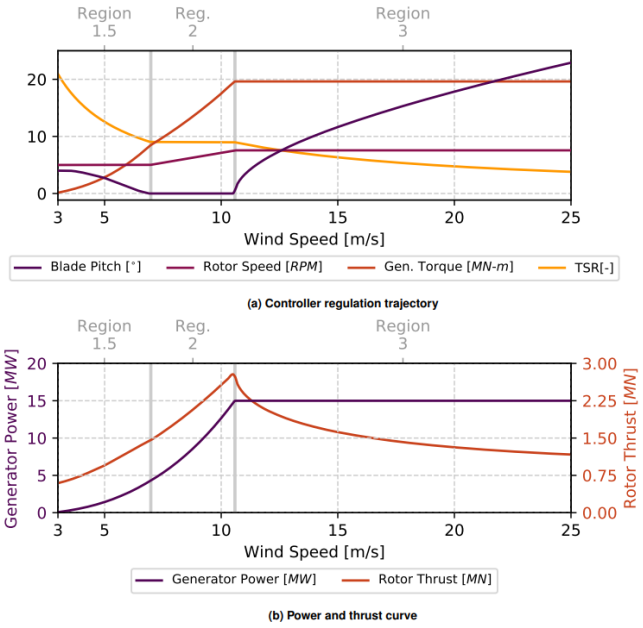

Figure 2. Performance and operation of the IEA Wind 15 MW reference wind turbine rotor with the ROSCO controller.

As mentioned, in this study the wind turbine is operated only in the full load region (region 3 in Fig. 2), where the tower suffers the most damage since the tower base bending moments increase with the mean wind speed. In this region, the torque controller is saturated at rated torque and the blade pitch PI controller pitches to feather to maintain rated rotor speed.

The required turbulent wind field for simulations is generated using TurbSim (Jonkman, 2009). The wind signal is configured with a mean wind speed of 22 m/s, a Kaimal turbulence spectrum with 2.5 m/s of standard deviation, and a power-law vertical shear with an exponent of 0.2. The sampling frequency is set to 125 Hz.

3. CONTROL METHODOLOGY

The proposed control scheme is shown in Fig. 3. It consists of two controllers: a CPC and an AGTC. The control actions of these controllers generate the pitch and torque signals. Since the wind turbine is assumed to operate in the full load region at its rated power, the generator torque T_g is initially fixed at its rated value. According to (1), the generated power can be maintained at its nominal value if the wind turbine speed is controlled at its rated value. The CPC maintains this speed at its nominal value, rejecting the wind speed changes. The CPC controller used in this work is based on ROSCO (NREL, 2019), which is the default controller for the OpenFAST implementation of the Reference NREL wind turbine RWT.

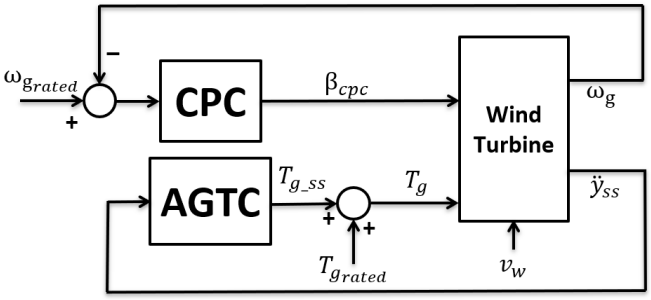

Figure 3. AGTC+CPC control scheme for the full load region.

The main control objective for AGTC is to minimize the structural loading of the side-side motion of the tower. To be more precise, the AGTC adds damping to the first natural frequency of tower side-side bending mode (about 0.2 Hz).

The AGTC produces an extra component $\tau_{g,SS}$ of the generator torque to be added to the rated torque, as shown in (2). This extra component is proportional to the nacelle side-side velocity. The final torque signal is constrained considering the slew rate and saturation limits of the generator. In most works, the extra component $\tau_{g,SS}$ is constrained to ±10% of the rated generator torque (Golnary & Tse, 2022). The lateral velocity can be obtained by measuring and integrating the tower-top side-side acceleration.

$$\tau_g = \tau_{g,rated} + \tau_{g,SS} = \tau_{g,rated} + k\dot{y}_{SS} \quad (2)$$

The AGTC scheme used in this work is shown in Fig. 4. Its parameters are the proportional gain k, derivative gain k_d (optional) and a second order bandpass filter (optional).

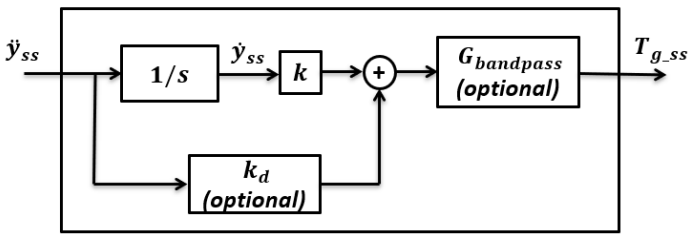

Figure 4. AGTC scheme.

Equation (3) shows the transfer function of the optional second order filter employed in our analysis:

$$G_{bandpass}(s) = \frac{2\xi\omega_n s}{s^2 + 2\xi\omega_n s + {\omega_n}^2} \quad (3)$$

where $\omega_n = 2\pi f_n$ characterizes the first natural frequency of the tower in the side-side direction, and ξ characterizes the corresponding damping ratio. This filter is aimed to limit the band of frequencies where AGTC should add damping so that unnecessary actions are avoided at other frequency ranges.

3.1 AGTC tuning via genetic algorithms

The proposed objective for the optimization is to minimize the tower fatigue loading through the side-side tower bending

moment M_{ss}. For fatigue assessment in wind turbines, the Fatigue Damage Equivalent Load (DEL) is usually calculated in the time domain using cycle counting techniques. To determine the fatigue damage of the tower base side-side, the DEL index based on the M_{ss} is calculated and employed as the objective function to be minimized. This function cannot be evaluated analytically since the DEL index is computed offline from the time series of simulation data, and the optimization procedure becomes a nonlinear problem that requires intensive computational effort and time. To achieve better computational efficiency (Serrano et al., 2022; Lara et al., 2021, 2022), the optimization is performed using genetic algorithms (GA). The tuning procedure of the AGTC control parameters is performed by simulating the wind turbine model IEA 15 MW RWT (see Table 1) in OpenFAST. The simulation data are subsequently post-processed with MLife (NREL, 2012) for the DEL calculation.

In the proposed optimization, the parameter sets are as follows: [k] for the case of AGTC-P, [k kd] for the case of AGTC-PD, and [k fc ε] for the case of AGTC-P plus filter. The search range for the gains is [0-10e8], the range for fc is [0.15-0.25] Hz, and [0.001-20] for ε. The main options configured in the genetic algorithm are a population size of 300, elite count of 0.05 times the population size for reproduction with a crossover fraction of 0.8.

Table 2 shows the control parameters obtained for the various AGTC versions after optimization.

Table 2. Optimized parameters for the AGTC

Scheme	k (N·s)	k_d (N·s^2)	f_c (Hz)	ε
AGTC-P	8.80e6	-	-	-
AGTC-PD	8.65e6	6.72e5	-	-
AGTC-P+Filter	35.89e6	-	0.21	0.63

4. RESULTS

This section analyzes the simulation results of the proposed AGTC controllers tuned with the previous optimal parameters shown in Table 2. Table 3 shows the DEL indices of M_{ss} obtained from the optimal solutions, the standard deviations of the torque signal, the generated power, the side-side displacement and the total variation (TV) of the torque according to the following equation:

$$TV_{T_g} = \frac{1}{t_n - t_0} \sum_{k=1}^{n} \left| T_g(t_k) - T_g(t_{k-1}) \right| \quad (4)$$

The absolute value is shown as well as the percentage relative to the baseline case (i.e., the ROSCO controller without any AGTC strategy). For example, the AGTC-P controller decreases the DEL index a value of -34.55% in comparison with that of the baseline case.

Figures 5 and 6 show the times responses of the analyzed control strategies, including the baseline ROSCO controller. The plots show the wind speed, the generated power, the generator speed, the tower side-side displacement, the tower base side-side moment, and the generator torque. As can be seen, the displacements are reduced with any of the AGTC strategies. In all the AGTC schemes, the DEL index is reduced more than 30%. This reduction is expected according to the third plot of Figs. 5-6, where the M_{ss} amplitudes of the AGTC strategies are significantly smaller than those of the baseline case. It is interesting to note that the AGTC-P+Filter controller obtains the best performance for x_{ss} and DEL function. However, this result is achieved at the expense of a higher standard deviation in the generated power, which is increased from 6.33% (AGTC-P scheme) to 23.28%.

Table 3. DEL cost function and performance indices

Scheme	DEL (M_{ss})	TV_{Tg}	STD_{xss}	STD_{Tg}	STD_{Pg}
Baseline CPC	5.47e4	0	0.0743	0	794.51
AGTC-P	3.58e4 (-34.55%)	1760	0.0371 (-50.06%)	383.96	844.83 (+6.33%)
AGTC-PD	3.39e4 (-38.02%)	3416.7	0.0373 (-49.79%)	398.61	849.38 (+6.90%)
AGTC-P+Filter	3.13e4 (-42.77%)	1091.7	0.0330 (-55.58%)	761.97	979.44 (+23.28%)

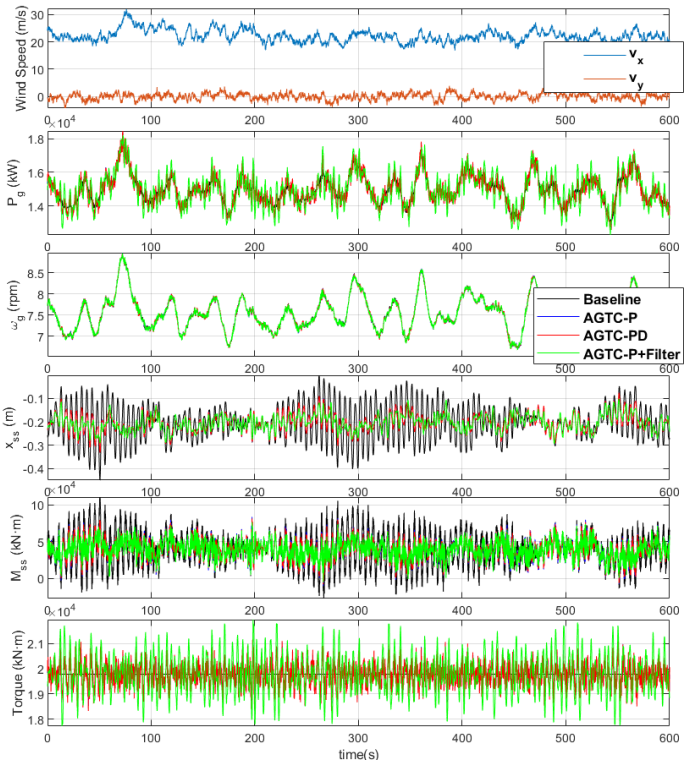

Figure 5. Time responses of the wind speed, generated power, generator speed, tower side-side displacements, tower base side-side moment and generator torque.

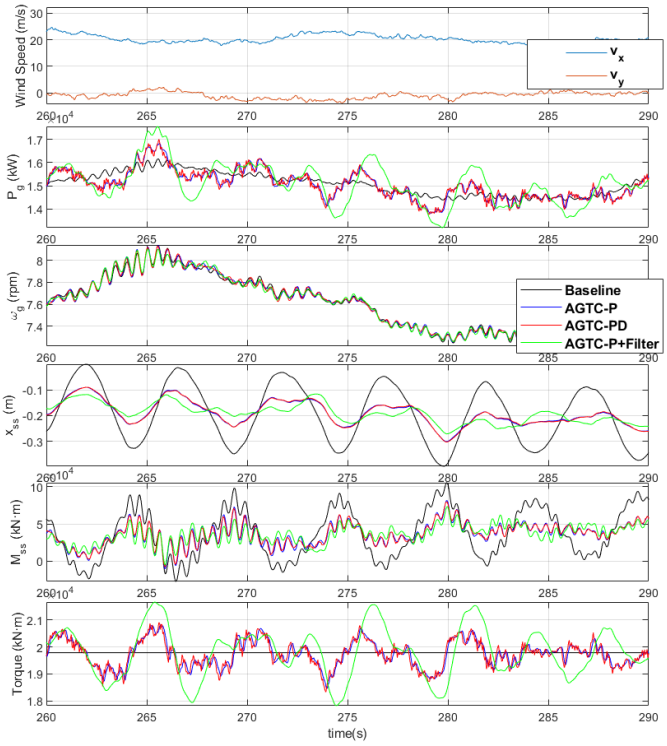

Figure 6. Zoomed time responses of the wind speed, generated power, generator speed, tower side-side displacement, tower base side-side moment and generator torque.

In addition, the use of a filter smooths out the changes in the torque signal. This can be seen in the last plot of Fig. 6 for the AGTC-P+Filter option. While the torque signal has a larger amplitude, its changes are smooth, resulting in a value of 1091.7 in the TV_{Tg} index, the smallest of all the AGTC strategies.

Figures 7 and 8 show the Fourier spectra of the tower side-side displacement and bending moment. The first side-side tower bending mode is appreciated at 0.2 Hz. The AGTC-P and the AGTC-PD curves are overlapped in both figures and the peak at 0.2 Hz is significantly smaller. This peak is removed with the AGTC-P+filter scheme.

To sum up, all the AGTC strategies reduce this peak significantly, and the mitigation is total when the filter is incorporated. This conclusion can be appreciated in both frequency and time domains.

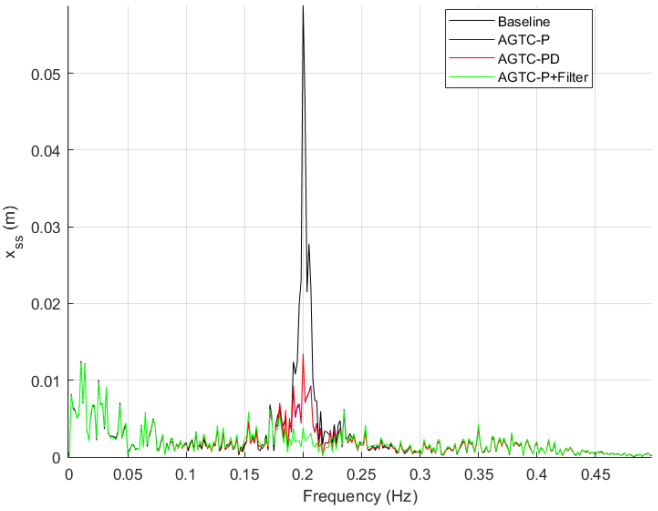

Figure 7. Fourier spectra of x_{ss}.

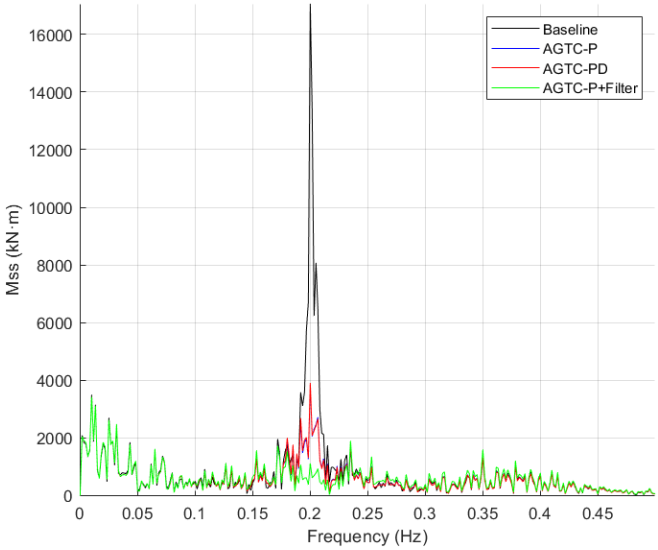

Figure 8. Fourier spectra of M_{ss}.

5. CONCLUSIONS

In this work, a control scheme is proposed for the mitigation of lateral tower vibrations in the full load region. The strategy combines an AGTC and a CPC scheme based on the NREL's Reference OpenSource Controller (ROSCO). Different configurations for the AGTC are proposed, including optional filters. The parameters are tuned through genetic algorithms, and the objective function to be minimized is based on the DEL index. The simulations are carried out with OpenFAST and the controllers are designed and applied to the IEA 15 MW RWT model. The controllers are compared with the baseline ROSCO controller. All the AGTC controllers mitigate significantly the lateral tower vibrations. There is a balance between reducing lateral oscillations of the tower and fluctuations in the output power, as changes in the generator torque causes variations in the output power. Future work will also apply these schemes to higher power wind turbines and will address the compromise between different conflicting

objectives, such as torque signal effort and tower load reduction, using multi-objective optimization.

ACKNOWLEDGEMENTS

This work was supported by the Spanish Ministry of Science and Innovation (MCIN/ AEI/10.13039/501100011033) under Grant PID2020-117063RB-I00 and jointly financed by the Operational Program of the European Regional Development Fund 2014-2020 and the Regional Ministry of Economic Transformation, Industry, Knowledge, and Universities of Andalusia, Spain, under Grant P18-TP-2040. M. Lara also expresses appreciation for the FPU fellowship (FPU17/02747) from the Spanish Ministry of Education, Culture, and Sports.

REFERENCES

Abbas, N. J., Zalkind, D. S., Pao, L., & Wright, A. (2022). A reference open-source controller for fixed and floating offshore wind turbines. *Wind Energy Science*, 7(1), 53-73. Available online: https://wes.copernicus.org/articles/7/53/2022 (accessed 1 June 2022).

Gambier, A., & Nazaruddin, Y. Y. (2022). Wind turbine pitch and active tower damping control using metaheuristic multi-objective bat optimization. *21st International Conference on Modeling and Applied Simulation*, MAS 2022.

Gambier, A. (2021). Pitch control of three bladed large wind energy converters— a review. Energies, 14(23), 1–24.

Jonkman, B. (2009). TurbSim user's guide: Version 1.50. Available at: https://www.osti.gov/biblio/965520 (accessed 1 December 2022).

Lackner, M. A., & Rotea, M. A. (2011). *Structural control of floating wind turbines*. Mechatronics, 21(4), 704-719.

Lara, M., Garrido, J., Ruz, M. L., & Vázquez, F. (2022). *Multi-objective optimization for simultaneously designing active control of vibrations and power control in wind turbines.* Accepted in December 2022 in Energy Reports.

Lara, M., Garrido, J., Ruz, M. L., & Vázquez, F. (2021). *Adaptive Pitch Controller of a Large-Scale Wind Turbine Using Multi-Objective Optimization*. Applied Sciences, 11(6), 2844.

Liu, X., Xu, J., He, G., & Chen, C. (2022). *Lateral vibration mitigation of monopile offshore wind turbines with a spring pendulum pounding tuned mass damper*. Ocean Engineering, 266.

Liu, H., Tang, Q., Chi, Y., Zhang, Z., & Yuan, X. (2016). *Vibration reduction strategy for wind turbine based on individual pitch control and torque damping control.* Transactions on Electrical Energy Systems, 26(10), 2230-2243.

Mensah, A.F., Dueñas-Osorio, L. "014). *Improved reliability of wind turbine towers with tuned liquid column dampers (TLCDs)*. Structural safety, 47, 78-86.

Niranjan, R., & Ramisetti, S. B. (2022). *Insights from detailed numerical investigation of 15 MW offshore semi-submersible wind turbine using aero-hydro-servo-elastic code*. Ocean Engineering, 251.

Njiri, J. G., & Söffker, D. (2016*). State-of-the-art in wind turbine control: Trends and challenges*. Renewable and Sustainable Energy Reviews, 60, 377-393.

Novaes Menezes, E. J., Araújo, A. M., & Bouchonneau da Silva, N. S. (2018). A review on wind turbine control and its associated methods. Journal of Cleaner Production, 174, 945–953.

Papi, F., & Bianchini, A. (2022). *Technical challenges in floating offshore wind turbine upscaling: A critical analysis based on the NREL 5 MW and IEA 15 MW reference turbines*. Renewable and Sustainable Energy Reviews, 162.

Serrano, C., Sierra-Garcia, J.-E., & Santos, M. (2022). *Hybrid Optimized Fuzzy Pitch Controller of a Floating Wind Turbine with Fatigue Analysis*. Journal of Marine Science and Engineering, 10(11), 1769.

Mohammadi, E., Fadaeinedjad, R., & Moschopoulos, G NREL. (2018). *Implementation of internal model based control and individual pitch control to reduce fatigue loads and tower vibrations in wind turbines*. Journal of Sound and Vibration, 421, 132-152.

NREL. (2020). *Definition of the IEA 15-Megawatt Offshore Reference Wind. National Renewable Energy Laboratory*. Available at: https://github.com/IEAWindTask37/IEA-15-240-RWT

NREL. (2019). *NREL's Reference OpenSource Controller (ROSCO) toolbox for wind turbine applications*. Available at: https://github.com/NREL/ROSCO

NWTC Information Portal. (2012). *MLife*. https://www.nrel.gov/wind/nwtc/mlife.html (accessed 28 december 2022)

OpenFAST v3.2.0 documentation (n.d.) OpenFAST. Available at: https://openfast.readthedocs.io/en/main/ (accessed 26 October 2022).

Zhang, Z., Staino, A., Basu, B., & Nielsen, S. R. (2016). *Performance evaluation of full-scale tuned liquid dampers (TLDs) for vibration control of large wind turbines using real-time hybrid testing*. Engineering Structures, 126, 417-431.

Zhang, Z., Nielsen, S. R., Blaabjerg, F., & Zhou, D. (2014). *Dynamics and control of lateral tower vibrations in offshore wind turbines by means of active generator torque*. Energies, 7(11), 7746-7772.

Zuo, H., Bi, K., & Hao, H. (2020). *A state-of-the-art review on the vibration mitigation of wind turbines*. Renewable and Sustainable Energy Reviews, 121.